Catalysis Today xxx (2017) xxx–xxx

Contents lists available at ScienceDirect

Catalysis Today

journal homepage: www.elsevier.com/locate/cattod

Synthesis of titanium containing MCM-41 from industrial hexafluorosilicic acid as epoxidation catalyst

Tieliang Liu, Fang Jin*, Xianqiao Wang, Yangchun Fan, Ming Yuan

Key Laboratory for Green Chemical Process of Ministry of Education, Hubei Novel Reactor & Green Chemical Technology Key Laboratory, School of Chemical Engineering and Pharmacy, Wuhan Institute of Technology, Wuhan, 430205, China

ARTICLE INFO

Article history:
Received 16 October 2016
Received in revised form 17 January 2017
Accepted 6 March 2017
Available online xxx

Keywords:
Mesopore
Molecular sieves
Hydrothermal
Epoxidation
Catalysis

ABSTRACT

The industrial by-product hexafluorosilicic acid was investigated as silicate source for titanium containing MCM-41 (Si/Ti–MCM-41) synthesis. An extended and detailed study, which includes the effects of several factors such as the state and content of Ti, surfactant/Si ratio and template removal technique on the physicochemical properties and catalytic activity of Si/Ti–MCM-41, is presented; The Si/Ti–MCM-41 was also characterized by powder X-ray diffraction, N_2 adsorption-desorption, fourier transform infrared spectroscopy, ultraviolet-visible spectrophotometer, thermal gravimetric measurements, X-ray fluorescence and scanning electron microscopy. The results show that the specific surface area and pore volume of the molecular sieve reach 1040 $m^2 g^{-1}$ and 0.74 $cm^3 g^{-1}$ under the hydrothermal conditions of the Si/Ti mole ratio equal to 60, CTAB/Si mole ratio to 0.81, hydrothermal temperature at 343 K and time for 3 h. The catalytic performance shows that samples have higher activity and selectivity for cyclohexene epoxidation to produce cyclohexene oxide. With the reaction temperature 333 K and mole ratio of cyclohexene/tertiary butyl peroxide hydrogen equal to 1, the highest cyclohexene conversion and epoxide selectivity is 79.23% and 95%, respectively. The catalyst activity has not obvious change with two times recycles.

© 2017 Elsevier B.V. All rights reserved.

1. Introduction

A huge amount of industrial hexafluorosilicic acid (H_2SiF_6) is generated annually as a by-product from phosphate fertilizer industries. The collection of 16–18 wt% H_2SiF_6 is normally carried out via the absorption process of gaseous silicon tetrafluoride (SiF_4) in the water scrubber. However, the industrial H_2SiF_6 solution with this concentration is difficult to industrial application. It has been used to produce low value-added products, such as fluorosilicate, fluoride salt or white carbon black. Moreover, these low value-added products sales are not good, leading to the SiF_4 recovery of low concentration of H_2SiF_6 backlog. Therefore, some factories are not willing to recover SiF_4. The direct emission of SiF_4 into the atmosphere would not only cause resources consumption but also give rise to environmental pollution. Waste water containing fluorine ions is great pollution to the environment, which endangers the health of animals and plants. More than 0.15 mg L^{-1} fluoride content in drinking water will cause bone and dental fluorosis diseases. Therefore, some researchers try to apply H_2SiF_6 or SiF_4 produced in the phosphate fertilizer industries as the raw material to produce some high value-added products, in order to boost the enthusiasm of the manufacturer to recycle silicon fluoride, reducing emissions of fluoride pollution to the environment. Yu et al. [1] reported that a high purity amorphous silica can be obtain through a two-step neutralization of H_2SiF_6 with ammonia. Sarawade et al. [2] produced HF and high specific surface area of silica with phosphoric acid by-product H_2SiF_6. Elineema et al. [3] reported the recovery of high purity nanoporous silica from H_2SiF_6 and Na_2SiO_3 from the phosphate fertilizer industry. Cicala et al. [4] synthesized amorphous silicon alloys from fluorinated gases by plasma deposition. Guzeev et al. [5] produced zircon and zirconium tetrafluoride with silicon tetrafluoride and zirconium dioxide as raw material.

Epoxide and its derivatives is one of the important intermediate of many chemical products such as pharmaceuticals, food additives, preservatives, etc. So the synthesis of epoxide and its derivatives are received wide attention. It has been shown that titanosilicates are the most efficient heterogeneous epoxidation catalysts. TS-1 exhibits high catalytic activity and selectivity in the epoxidation of propylene using aqueous H_2O_2 as an oxidant [6]. However, the steric limitation of its small pore opening restricts it to the epoxidation of non-linear alkenes. Therefore, the mesoporous titanosilicates have been developed to overcome the problem [7].

* Corresponding author.
E-mail address: fangjin@wit.edu.cn (F. Jin).

http://dx.doi.org/10.1016/j.cattod.2017.03.011
0920-5861/© 2017 Elsevier B.V. All rights reserved.

Please cite this article in press as: T. Liu, et al., Synthesis of titanium containing MCM-41 from industrial hexafluorosilicic acid as epoxidation catalyst, Catal. Today (2017), http://dx.doi.org/10.1016/j.cattod.2017.03.011

Mobil's researchers successfully synthesized a series of mesoporous material named M41S since 1992 [8]. Because its huge potential commercial value in the field of industrial catalysis and adsorption separation process, it has been the hotspot in research of various related disciplines [9–16]. The organic silicon source, such as titanium isopropoxide(TEOS), tetramethyl orthosilicate(TMOS) are conventional silica sources for the synthesis of mesoporous molecular sieve MCM-41 [17–19]. However, the expensive cost of organic silicon source for the synthesis of MCM-41 weighs heavily against it wide industrial application for the adsorption and catalysis. Therefore, researchers began to search cheap and extensive sources of silicon source to replace expensive organic silicon source. Lin et al. [20] utilized inorganic silicon source sodium silicate to synthesize hollow tubular morphology MCM-41. Antochshuk et al. [21] used fumed silica as raw material for MCM-41 and Ce-MCM-41 synthesis. Adjdir et al. [22] and Yang et al. [23] successfully synthesized MCM-41 with volclay and bentonite as silicon source, respectively.

We report a method that utilized phosphate fertilizer by-product H_2SiF_6 as the silicon source to synthesize titanium containing mesoporous molecular sieves as a catalyst. This method is supposed to be markedly profitable in the industrial aspect, because it can improve additional value of H_2SiF_6 and decrease the cost of synthesized MCM-41. Moreover, the synthetic process could be easily industrial application through hydrothermal treatment at atmosphere.

2. Experimental

2.1. Catalysts preparation

4 g cetyltrimethylammonium bromide (CTAB) were dissolved in 96 mL $NH_3{\cdot}H_2O$ to make the solution A; 0.4 g tetraisopropyl titanate ($Ti(OCH(CH_3)_2)_4$) (TTIP) was mixed with the 10 mL 35 wt% H_2O_2 as solution B. Then, 20 g 16 wt% H_2SiF_6 of phosphate fertilizer industrial by-product was added to solution A, stirred at 323 K. Then the solution B was also added to solution A. The mixture was hydrothermal treatment at 323–363 K for 1–5 h under stirring in a flask with the refluxing. The mole ratio of each composition in the reaction mixture is SiO_2: CTAB: TTIP: H_2O_2: NH_3: H_2O = 1:0.1–1.0:0.01–0.1:4.5:12:400. The hydrothermal product recovered by filtration, washed with distilled water and dried at a temperature of 333 K. The dried sample was named as-synthesized samples.

Two methods have been used to remove the CTAB surfactant from the as-synthesized samples. One was to calcinate sample under atmosphere at 813 K for 6 h, with a linear temperature ramp of 10 K min^{-1}. The resultant materials are designated as *x*Si/Ti–MCM-41, where *x* is the Si/Ti molar ratio in the reaction mixture. The other one was to remove surfactant from the as-synthesized samples by the extraction method. The dried as-synthesis sample was refluxed in 100 mL 1.2, 2.4 mol L^{-1} hydrochloric acid anhydrous ethanol solution (HCl/ethanol solvent) under stirring for 1 h. This material was immediately filtered, washed with ethanol and dried at 353 K overnight. The resultant materials are designated as *y*A-*x*Si/Ti–MCM-41, where *y* is 1.2 or 2.4, which is assigned as the concentration of acid solution.

2.2. Catalysts characterization

The low angle region X-ray diffraction (XRD) patterns were obtained on D/max 2200PC using Cu–K_α radiation (k = 0.154 nm). The instrument was operated at 40 kV and 30 mA. The scanning range is from 1.5 to 10°. N_2 ad/desorption measurements were carried out on Micromeritics VII2390 apparatus at 77 K. Prior to the analysis, the samples were degassed at 373 K under nitrogen purging for 1 h, then at 373 K under nitrogen purging for 1 h. The specific surface area was calculated by the Brunauer-Emmett-Teller (BET) method in the 0.05–0.25 P/P_0 range. The pore volumes and their size distributions were derived from the desorption branch of the N_2 isotherms using the Barrett-Joyner-Halenda (BJH) method. The Shimadzu UV-3000 type double wavelength solid ultraviolet-visible spectrophotometer (UV–vis) determines of Ti the coordination number of the atom. Transmission electron microscopy (TEM) was carried out on a HITACHIS 23200N instrument using an electron beam. The TG-DTG curve of MCM-41 was characterized by a Mettler TGA/SDTA851 thermal gravimetric analyzer at a rate of 10 K min^{-1} in the range of 273–1073 K. Chemical analysis was performed for Si and Ti by Energy Dispersive Spectroscopy (EDS) of Vario EL III CHNSO. Fourier Transform infrared spectroscopy (FTIR) spectra of solid samples were collected in a Nicolet Magna IR 750 spectrometer using a KBr pellet technique, with 2 mg sample diluted with 100 mg of KBr and shaped into a 10 mm o.d. pellet. X-Ray Fluorescence (XRF) Spectrometers of solid samples were collected in Bruker AXS of S4 Pioneer with standardless quantitative analysis method.

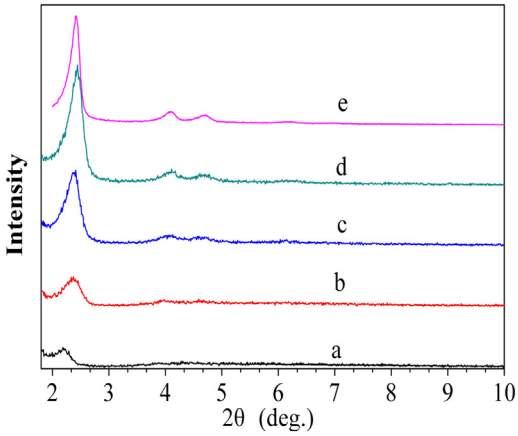

Fig. 1. XRD patterns of *x*Si/Ti-MCM-41 samples synthesized with different Si/Ti molar ratios(a) 10, (b) 30, (c) 60 and (d)120, (e) ∞.

2.3. Catalytic reaction

The catalytic activities of *x*Si/Ti–MCM-41 materials were examined by carrying out liquid phase epoxidation of cyclohexene with tert-butyl hydroperoxide (TBHP) (1.2 mol L^{-1} in decane) at 333 K. Calcined *x*Si/Ti–MCM-41 samples were pre-dried at 353 K overnight before using as the catalyst. In a typical run, a mixture of 10 mmol cyclohexene, 10 mmol TBHP, 50 mg of the catalyst in powder form were heated at 353 K in a necked round bottom flask with a stir bar stirring at 200 r.p.m. and cooling condenser to reflux for 5 h. Then the reaction mixtures were collected by the removal of solid catalysts and then qualitatively analyzed by a gas chromatograph (GC) equipped with KB-Plot Q capillary column and FID detector, where benzene was used as an internal standard. The cyclohexene conversion and product selectivity were calculated by the following equations.

$$Conversion(\%) = (formed\ derivatives\ of\ cyclohexene\ in\ mol/initial\ cyclohexene\ in\ mol) \times 100.$$

$$Selectivity(\%) = (specific\ product\ in\ mol/formed\ derivatives\ of\ cyclohexene\ in\ mol) \times 100.$$

Please cite this article in press as: T. Liu, et al., Synthesis of titanium containing MCM-41 from industrial hexafluorosilicic acid as epoxidation catalyst, Catal. Today (2017), http://dx.doi.org/10.1016/j.cattod.2017.03.011

3. Results and discussion

3.1. The influence of Ti content on the pore structure of xSi/Ti–MCM-41

As shown in Table 1, the XRF analysis results of the synthesized *x*Si/Ti–MCM-41samples indicate their Si/Ti molar ratios are closed to those of corresponding hydrothermal mixtures, which indicates that most of Ti added in the hydrothermal process has been incorporated into *x*Si/Ti–MCM-41. Because the industrial fluosilicate are used as silicon source to synthesize mesoporous molecular sieves, which contains the impurities such as Fe, Al, Na, etc., the produced mesoporous molecular sieve contains some impurities. Besides the impurities of fluorine (about 2.9 wt%), it also contains other trace amount of Fe, Al, Na and K. The content of impurities of XRF characterization results are shown in Table 1. Moreover, the content of the impurities are almost constant in the produced mesoporous titanosilicate with different Si/Ti ratio.

The XRD patterns of *x*Si/Ti–MCM-41 with different Si/Ti molar ratios are show in Fig. 1. The (*100*), (*110*), (*200*) and (*210*) diffraction peaks in the XRD pattern of samples show highly ordered MCM-41 hexagonal *p6 mm* structure [24]. It can be seen that the peaks intensity is gradually reduced with the decrease of Si/Ti molar ratios from 120 to 10. Moreover, the characteristic peak intensities of Si/Ti–MCM-41 with different Si/Ti molar ratios are lower than pure siliceous MCM-41. The interplanar distance (d_{100}) and the hexagonal unit cell parameter ($a_0 = 2d_{100}/\sqrt{3}$) of the samples were estimated from the (*100*) position of the XRD diffraction peak, and presented in Table 1 [25]. The d_{100} values were reported to be very sensitive to the degree of organization order of the product [25,26]. Because the [TO_4] cell is bigger than [SO_4] unit, the incorporation of [TO_4] into the mesoporous molecular sieve would make the [TO_4] surrounding lattice expansion and the hexagonal unit cell parameter (a_0) become bigger [23]. It can be observed that the (*100*) reflection peak move slightly to lower angle with the increase of the Ti content in the *x*Si/Ti–MCM-41, which means that the d_{100} spacing, lattice parameter (a_0) and the wall thickness of the hexagonal mesopores *t* increase concurrently. Therefore, it demonstrates that the Si/Ti ratio can influence the packing of the silicon and consequently the degree of long-order structure of MCM-41.

TEM micrographs of calcined *60*Ti/Si–MCM-41 are given in Fig. 2. The images of the sample presents a well-defined hexagonal arrangement with a fairly uniform pore structure. The Fig. 2 shows that addition of titanium influences the structure of Si/Ti–MCM-41. Overloaded titanium ruined the highly ordered MCM-41 hexagonal *p6 mm* crystal structure, but this damage is not throughout the crystal structure. This behavior, the presence of disordered regions, lamellar phases, and fingerprint-like structures, has been reported in the literature for MCM-41 synthesis [27].

The N_2 ad/desorption isotherm was studied to evaluate the mesoporous structures of samples Si/Ti–MCM-41. A typical reversible type IV ad/desorption isotherm for mesoporous solids are observed as shown in Fig. 3. N_2 ad/desorption curve of these samples shows the same trend. At low relative pressure ($P/P_0 < 0.2$) the N_2 sorption update amount is smoothness, which is corresponding to N_2 adsorbs on the walls of the mesoporous in Si/Ti–MCM-41 samples. A marked inflection is perceived between the relative pressures (P/P_0) of 0.2–0.4, which is corresponding narrow and uniform pore size distribution band in the pore size distribution (PSD) curve, as shown in the BJH PSD curves of Fig. 3 [12,28,14]. This is caused by capillary condensation during the adsorption step and is an indication of the mesoporosity of the samples. The sample *120*Si/Ti–MCM-41, *60*Si/Ti–MCM-41 and *30*Si/Ti–MCM-41 have a great marked inflection in the relative pressures (P/P_0) of 0.2–0.4. However, with the increase of titanium content to Si/Ti ratio of 10, the PSD curves inflection of *10*Si/Ti–MCM-41 is much weaker which indicates that the pore structure of this sample is not as good order as others. The pore sizes are calculated by the BJH method from the desorption isotherm branch [29]. The mesoporous pore size of *120*Si/Ti–MCM-41, *60*Si/Ti–MCM-41, *30*Si/Ti–MCM-41, *10*Si/Ti–MCM-41 are about 2.5 nm, which does not change significantly with the increase of titanium content. N_2 ad/desorption curve shows hysteresis loop in the relative pressure (P/P_0) of 0.4–1.0, the hysteresis loop expanded with the increase of titanium content. This phenomenon can be attributed to the length of Ti-O bond is longer than that of Si-O bonds, and the addition of extra amount of titanium can partly damage pore wall of mesopore structure, which makes the pore wall produce defect [30]. As shown in Table 1, the values of surface areas and pore volume of *120*Si/Ti–MCM-41, *60*Si/Ti–MCM-41 and *30*Si/Ti–MCM-41 are closed to each other, which are significantly higher than those of *10*Si/Ti–MCM-41. This can be attributed to that the increase of titanium contents deteriorates the mesoporous structure of MCM-41. It has been reported that when the titanium contents are greater than 3.7 wt%, the hexagonal *p6 mm* structure of MCM-41is lost [28].

3.2. The influence of Si/Ti ratio on the coordination state of incorporated Ti

UV-vis diffuse reflectance spectroscopy is an effective means for characterization of titanium coordination number of the incorporated Ti species in the synthesis samples as shown in Fig. 4. According to the literatures [14,31], absorption peaks at 220 nm are corresponding to four coordination of titanium; Absorption peak at 260 nm is assigned to six coordination corresponding titanium; Absorption peak at 300 nm is the characteristic peak of anatase or rutile titanium oxide. The sample *120*Si/Ti–MCM-41 has only one absorption peak at 220 nm, inferring that all Ti species are in tetrahedral (T_d) coordination. Sample *60*Si/Ti–MCM-41, *30*Si/Ti–MCM-41 have a sharp absorption peak around 220 nm and a shoulder peak at 260 nm, indicating that most of Ti(IV) cations are in T_d coordination but a small portion presents in octahedral (O_h) coordination. Sample *10*Si/Ti–MCM-41 has a pronounced absorption bond at about 260 nm, which extends to the range above 300 nm, inferring that the Ti(IV) cations in this sample are mainly O_h coordination with the formation of TiO_2 clusters or crystallites. These results demonstrate that better dispersion of Ti(IV) is achieved by reduce the addition amount of titanium in the synthesized samples.

3.3. The influence of hydrothermal conditions on the pore structure of 60Si/Ti–MCM-41

The CTAB/Si mole ratio can greatly influent the mesoporous structure of *60*Si/Ti–MCM-41. The N_2 ad/desorption and pore size distribution curves of the samples with different CTAB/Si mole ratio are shown in Fig. 5. With the relative pressure P/P_0 in the range between 0.25–0.35, a dramatic increase of N_2 absorption occurs for the three samples, which is the character of the N_2 sorption isotherm of titanosilicate MCM-41 with mesopore about 2 nm. The data of samples 1, 2 & 3 in Table 2 shows that the pore structure of these samples change with the increase of CTAB contents, while with the CTAB/Si ratio 0.81 the specific surface area and pore volumes reaches the largest value among these samples. The XRD patterns in Fig. 6 indicate that the synthesized *60*Si/Ti–MCM-41 samples with different CTAB/Si mole ratio are also preserve the hexagonal *p6 mm* structures.

Please cite this article in press as: T. Liu, et al., Synthesis of titanium containing MCM-41 from industrial hexafluorosilicic acid as epoxidation catalyst, Catal. Today (2017), http://dx.doi.org/10.1016/j.cattod.2017.03.011

Table 1
Physical properties of synthesized xSi/Ti-MCM-41.

Sample	Si/Ti atomic ratio[a]	Ti (wt%) [a]	F (wt%) [a]	Al (wt%)	S_{BET} ($m^2\ g^{-1}$)	V_{meso}[b] ($cm^3\ g^{-1}$)	2θ	d_{100}[c] (nm)	a_0[d] (nm)	d_p[e] (nm)	t[f]
*10*Si/Ti-MCM-41	9	8.34	2.85	1.86	896	0.51	2.25	3.92	4.56	2.34	2.22
*30*Si/Ti-MCM-41	40	2.03	2.98	1.78	1011	0.73	2.36	3.73	4.31	2.36	1.95
*60*Si/Ti-MCM-41	77	1.39	2.89	1.46	992	0.7	2.4	3.68	4.25	2.38	1.87
*120*Si/Ti-MCM-41	150	0.62	2.99	1.78	1001	0.72	2.46	3.58	4.16	2.4	1.76

[a] XRF analysis results of calcined samples, Samples contains other trace impurities, Fe wt%:0.43-0.44; Na wt%: 0.25–0.32; K wt%:0.04–0.18.
[b] The mesopore volume (V_{meso}) is calculated from *t*-plot method.
[c] d_{100}: d spacing, the space distance between *(100)* planes.
[d] a_0: lattice cell parameter of the hexagonal structure.
[e] d_p: pore diameter calculated from the main peak of the BJH pore diameter distribution profile.
[f] $t = a_0 - d_p$:the wall thickness of the hexagonal mesopores.

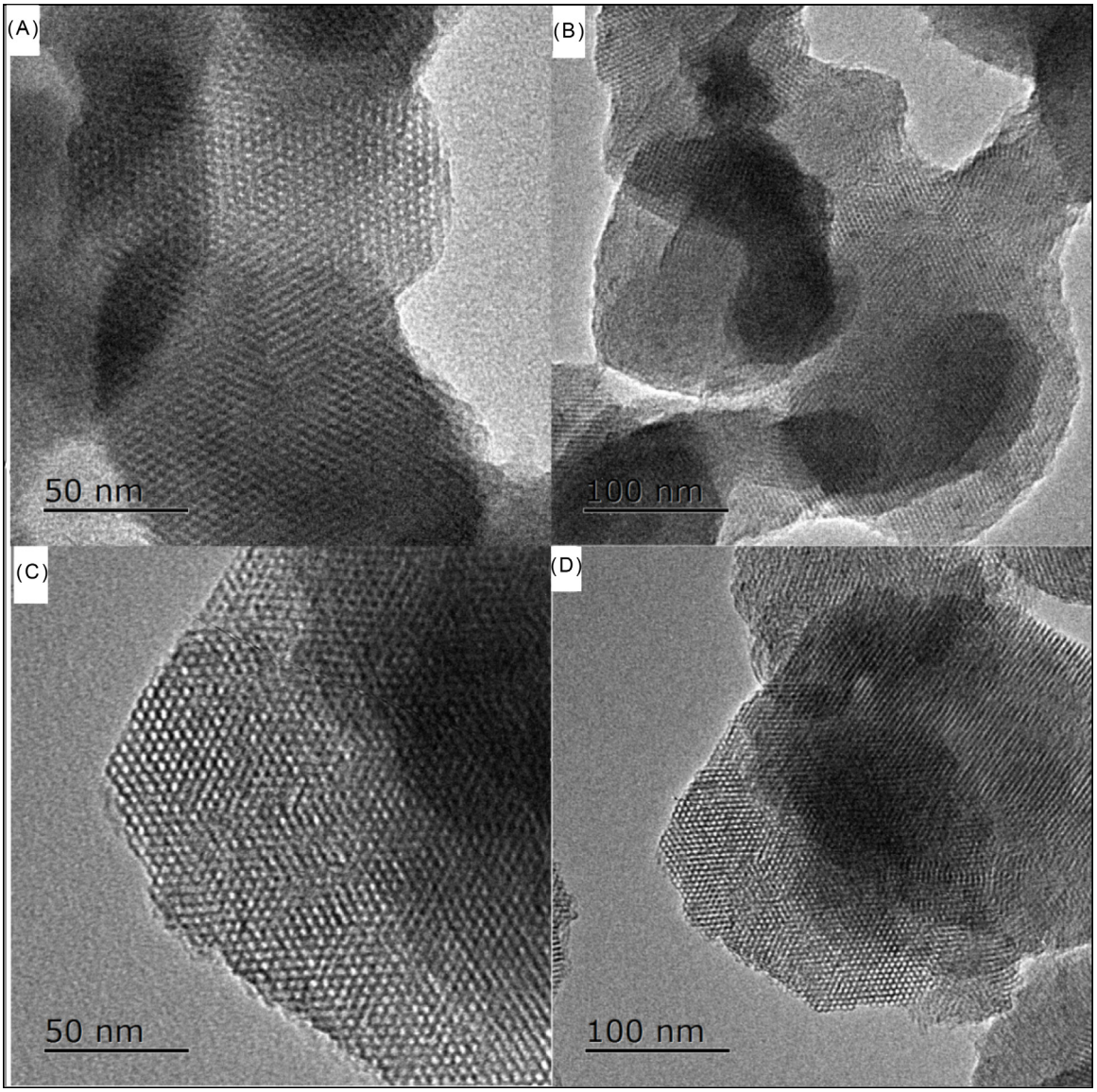

Fig. 2. TEM micrographs of *x*Si/Ti-MCM-41 (A) & (B) for $x = 10$, (C) & (D) for $x = 60$.

Hydrothermal temperature and time are also important factors to influence the structure of MCM-41 in the process of synthesis. With the Si/Ti molar ratio of hydrothermal precursor gel equal to 60, the influences of hydrothermal temperature and time on the textural properties of Si/Ti–MCM-41 samples were examined by N_2 physisorption as illustrated in Figs. 7 and 8. The N_2 ad/desorption isotherms of all samples synthesized with different hydrothermal temperature and time are all belong to type IV of IUPAC standards. The isotherm has a inflection point in P/P_0 0.2 and sharp increase in P/P_0 0.2–0.4, then the ad/desorption isotherms discover a platform, which indicates that the 2 nm mesopore structure of MCM-41 can be produced under these condition regions [25]. As the hydrother-

Please cite this article in press as: T. Liu, et al., Synthesis of titanium containing MCM-41 from industrial hexafluorosilicic acid as epoxidation catalyst, Catal. Today (2017), http://dx.doi.org/10.1016/j.cattod.2017.03.011

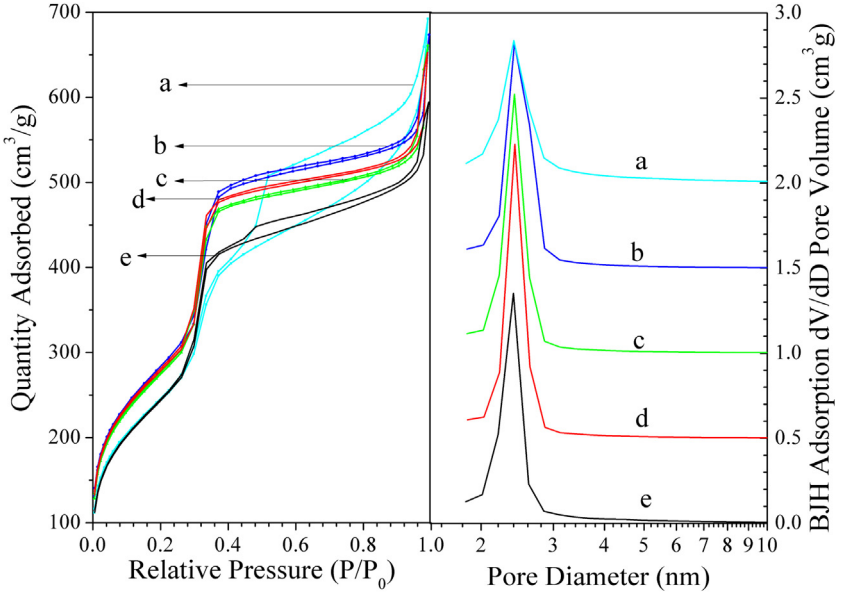

Fig. 3. N_2 ad/desorption isotherms of *x*Si/Ti-MCM-41(a) 10, (b) 30, (c) 60, (d)120 and (e) ∞.

Table 2
The surface area and pore volume of *60*Si/Ti-MCM-41 synthesized with different CTAB/Si ratio and same Si/Ti ratio and direct calcinations.

No.	CTAB/Si ratio of sample	Hydrothermal time(h)	Hydrothermal temperature(*K*)	*V*meso($cm^3\ g^{-1}$)	*S*BET ($m^2\ g^{-1}$)
1	1.62	3	343	0.62	988
2	0.81	3	343	0.74	1030
3	0.54	3	343	0.70	992
4	0.54	3	323	0.50	699
5	0.54	3	363	0.61	585
6	0.54	5h	343	0.50	699
7	0.54	1h	343	0.61	585

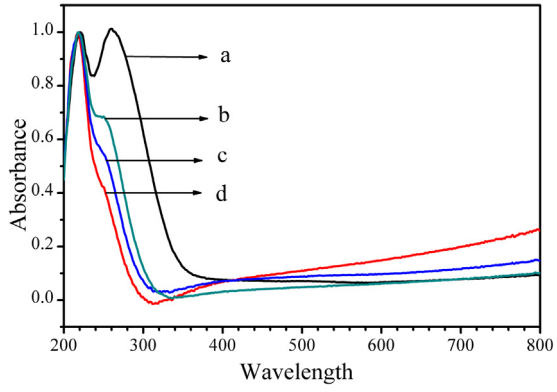

Fig. 4. DR UV-vis spectra of samples *x*Si/Ti-MCM-41 with different Si/Ti ratio (a) 10, (b) 30, (c) 60 and (d)120.

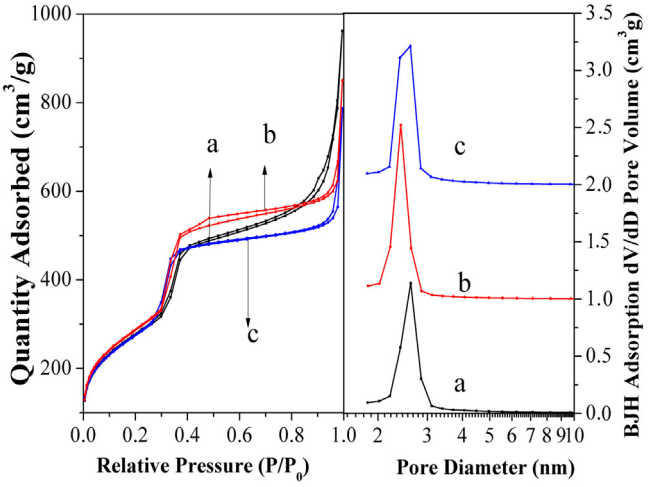

Fig. 5. N_2 ad/desorption isotherms of *60*Si/Ti-MCM-41 synthesized with different CTAB/Si ratio (a) 1.62, (b) 0.81, (c) 0.54.

mal temperature and time increases, the surface area of samples has the maximum as shown in Table 2 by comparison of the sample 3, 4, 5, 6, and 7. The maximum surface area of the 60Si/Ti–MCM-41 can reach 1030 $m^2\ g^{-1}$ under the hydrothermal condition of 343 K and 3 h. These phenomena indicate the temperature and time has great influence on the hydrothermal process.

3.4. Influence of surfactant removing method on the structure of xSi/Ti–MCM-41

The Si/Ti–MCM-41 as-synthesized and the samples after acid treatment or direct calcinations were studied by TG-DTG analysis. The results are indicated in Fig. 9. There is the significant weight loss for all the four curves below 373 K, which proves that weight loss is contributed to the evaporation of moisture contained in the sample [25]. In comparison, two distinct peaks have been founded at 523 K and 773 K for the sample of as-synthesized *60*Si/Ti–MCM-41. The curve of the sample *1.2*A-*60*Si/Ti–MCM-41 with lower concentration acid treatment shows the similar peak at 523 K, while the intensity of peak at 773 K significantly decreases compared with as-synthesized sample. The curves of the samples with higher acid concentration treatment, *2.4*A-*60*Si/Ti–MCM-41 and the sam-

Please cite this article in press as: T. Liu, et al., Synthesis of titanium containing MCM-41 from industrial hexafluorosilicic acid as epoxidation catalyst, Catal. Today (2017), http://dx.doi.org/10.1016/j.cattod.2017.03.011

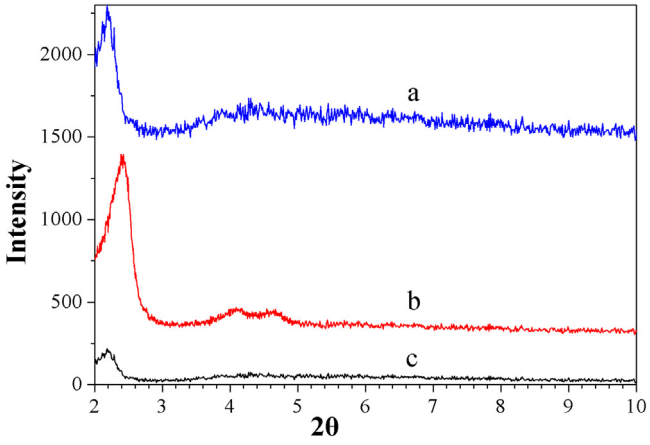

Fig. 6. XRD of *x*Si/Ti-MCM-41 synthesized with different CTAB/Si ratio (a) 1.62, (b) 0.81 and (c) 0.54.

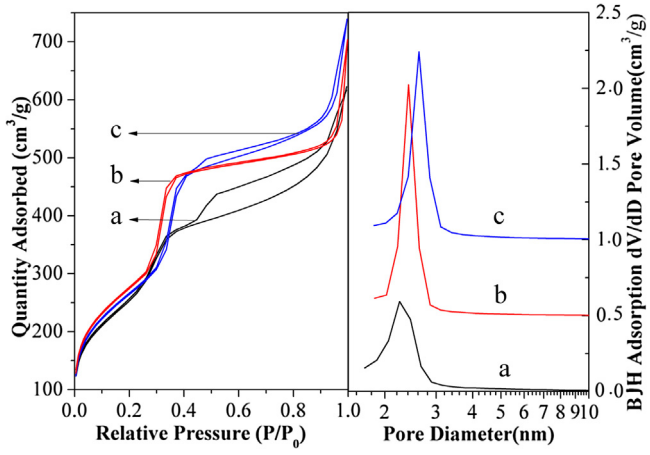

Fig. 7. N_2 ad/desorption isotherms of *60*Si/Ti-MCM-41 hydrothermal synthesized at difference temperature (a) 323 K, (b)343 K, (c)363 K.

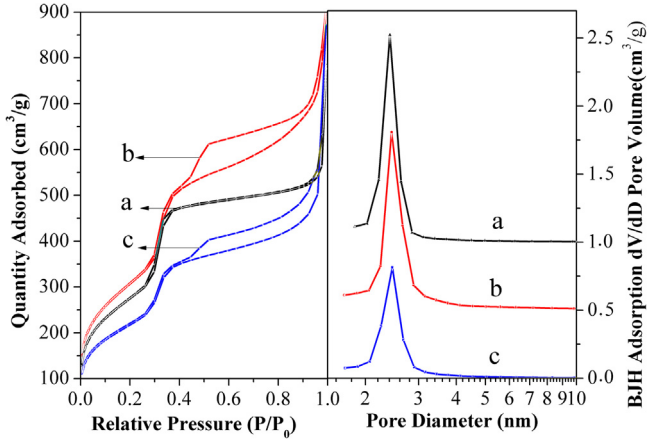

Fig. 8. N_2 ad/desorption isotherms of *60*Si/Ti-MCM-41 with difference hydrothermal time (a) 5 h, (b) 3 h, (c) 1 h.

ple after direct calcinations 60Si/Ti–MCM-41 appear no peaks at 523 K and 773 K. It has been reported that the complete removing of the template agent required calcinations temperature upon 773 K [19]. Therefore, the weight loss of samples in the TG test during 523 K and 773 K are deduced to be original from removing the template agent CTAB. It was reported that the CTAB attached to the surface of silicate-surfactant rods are relatively easy to be

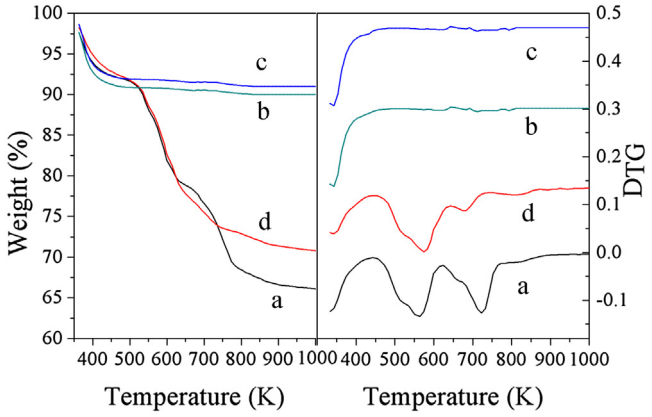

Fig. 9. The TG and DTG curves of the *60*Si/Ti-MCM-41 samples with (a) as-synthesized, (b) calcinated sample and acid treated samples with different acid concentration (c) 2.4 mol L^{-1} and (d) 1.2 mol L^{-1}.

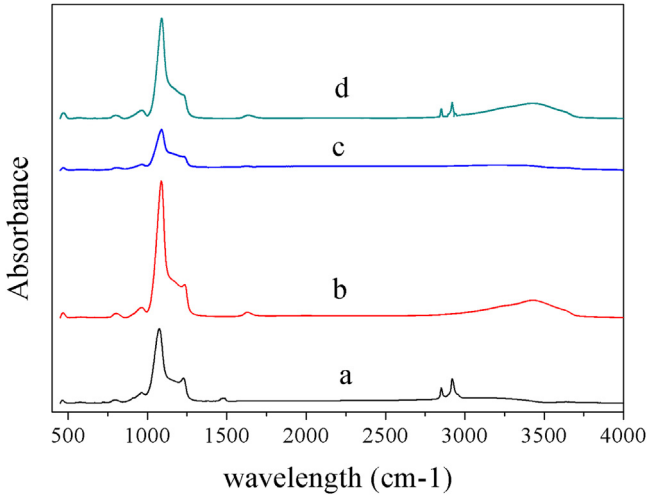

Fig. 10. The FTIR curves of the *60*Si/Ti-MCM-41 samples with (a) as-synthesized, (b) calcinated sample and acid treated samples with different acid concentration (c) 2.4 mol L^{-1} and (d) 1.2 mol L^{-1}.

burned at 523 K, while those trapped in mesoporous are needed to be removed above 773 K calcinations [32].

The as-synthesized and different post-processing *60*Si/Ti–MCM-41samples were also studied by FTIR analysis. The results were shown in Fig. 10. The as-synthesized and 1.2 mol L^{-1} acid treated samples have an absorption peak in the wavelength of 500–1750 and 2750–3000 cm^{-1}, while the calcinated and 2.4 mol L^{-1} acid treated samples only own the absorption peak in wavelength of 500–1750 cm^{-1}. It was reported that the vibration peaks of Ti—O—Si, Si—O—Si and Si—OH bonds belonging to the structure of titanosilicate are in the rage of 500–1750 cm^{-1} wavelength, while the absorption peak of C—H and C—C bound of templates is in the range of 2750–3000 cm^{-1} wavelength [33]. These results suggest that the as-synthesized and 1.2 mol L^{-1} acid treated samples still contain part of templates, and the calcinated and 2.4 mol L^{-1} acid treated samples have no template. These results are consistent with the results of TG-DTG. Therefore, it can be found that the templates in the as-synthesized Si/Ti–MCM-41 cannot be completely removed by low concentration 1.2 mol L^{-1} acid treatment. After increasing the acid concentration to 2.4 mol L^{-1} the templates in Si/Ti–MCM-41 can be completely removed. It has been reported that acid ethanol solution washing can remove the templates of molecular sieve precursor [13,34]. The acid treatment can decrease the interaction of temple with silicate, then the temples

Please cite this article in press as: T. Liu, et al., Synthesis of titanium containing MCM-41 from industrial hexafluorosilicic acid as epoxidation catalyst, Catal. Today (2017), http://dx.doi.org/10.1016/j.cattod.2017.03.011

Table 3
Influence of surfactant removing method on the pore structure of samples.

Sample name	V_{meso}/cm^3 g^{-1}	S_{BET}/m^2 g^{-1}
*1.2*A-*60*Si/Ti-MCM-41	0.59	887
*2.4*A-*60*Si/Ti-MCM-41	0.74	1040
60Si/Ti-MCM-41	0.70	992

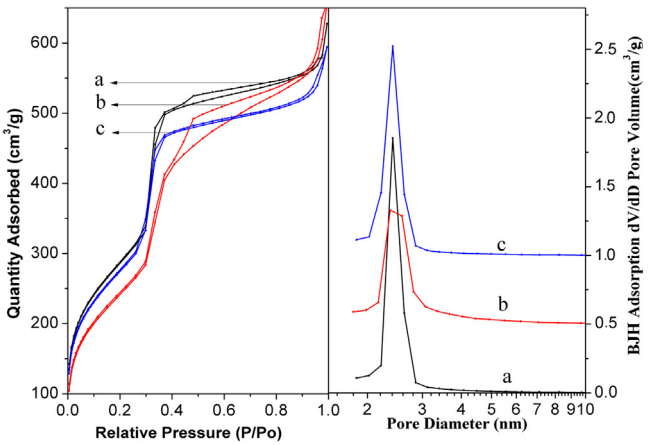

Fig. 11. The N_2 ad/desorption curve (A) and pore size distribution curves (B) for the samples with acid treatment (a) 2.4 mol L^{-1} (b) 1.2 mol L^{-1} and (c) calcination.

Table 4
Catalytic cyclohexene epoxidation performance.

Sample	$X_{Cyclohexene}$/%	S_{CHE}/%	S_{OH}/%	S_{ONE}/%	S_{CHD}/%
*120*Si/Ti-MCM-41	42.11	98.11	0.50	0.81	0.80
*60*Si/Ti-MCM-41	68.10	96.60	1.21	1.07	1.10
*2.4*A-*60*Si/Ti-MCM-41	64.35	95.09	1.01	1.69	2.21
*30*Si/Ti-MCM-41	59.14	95.94	0.72	1.72	1.62
*10*Si/Ti-MCM-41	46.62	89.49	1.10	6.72	2.69

$X_{Cyclohexene}$: Cyclohexene conversion; S_{CHE}: epoxy cyclohexane selectivity; S_{OH}:Cyclohexene alcohol selectivity; S_{ONE}: Ketone of cyclohexene selectivity; S_{CHD}:Cyclohexene diol selectivity.

resolve in the ethanol solution which is extracted from the pore of Si/Ti–MCM-41.

The N_2 ad/desorption are used to analysize and compare the pore structure of the two samples with CTAB removing by calcination or acid treatment. The specific surface area and pore volume for the sample *1.2*A-*60*Si/Ti–MCM-41 are relatively smaller with comparison with other two samples *2.4*A-*60*Si/Ti–MCM-41, *60*Si/Ti–MCM-41 due to incomplete remove of surfactant CTAB, which are presented in Table 3 and Fig. 11 are coincident with the TG and FTIR analysis results. The data of specific surface area and pore volume of *2.4*A-*60*Si/Ti–MCM-41 is slightly larger than that of calcinated sample *60*Si/Ti–MCM-41, indicating that the 2.4 mol L^{-1} HCl/ethanol solvent treatment can not only remove the surfactant but also avoid the damage of pore structure during calcinations.

3.5. Catalytic activity performance of different xSi/Ti–MCM-41

The success in preparation of Si/Ti–MCM-41 with H_2SiF_6 encouraged us to investigate its catalytic behaviors in the oxidation of bulky molecules. The cyclohexene epoxidation with TBHP was performed in decane solution at 333 K. The catalytic results after 5 h reaction are tabulated in Table 4. Fig. 12 illustrates the possible reaction mechanism of cyclohexene epoxidation over Si/Ti–MCM-41. Cyclohexene epoxide (CHE) is the target product. The hydrolysis of CHE may be catalyzed by acidic sites, resulting in 1, 2-cyclohexanediol(CHD) as a side product. The other side

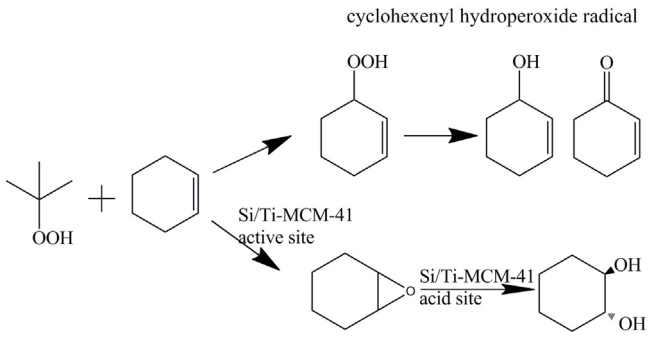

Fig. 12. The products of cyclohexene epoxidation over Si/Ti-MCM-41.

products 2-cyclohexen-1-ol(OH) and 2-cyclohexen-1-one (ONE) are formed through the cyclohexenyl hydroperoxide radical [12].

The results of cyclohexene epoxidation for different catalyst samples are shown in Table 4 to compare the activities of the samples *x*Si/Ti–MCM-41. With the increase of Si/Ti molar ratio, the conversion of cyclohexene increases firstly and then decreases. This result could be attributed to both the amount of active titanium active sites and coordination state of Titanium incorporated in the sample. When the titanium contents are not higher in the sample, the titanium(IV) is incorporated in the Si/Ti–MCM-41 structure with T_d coordination as epoxidation active sites. However, when the amount of titanium excessively increases in the *x* Si/Ti–MCM-41 with decrease of Si/Ti ratio, the T_d Ti active sites for epoxidation are transferred to the O_h Ti by polymerized, which has low activity for catalysis epoxidation. The *60*Si/Ti–MCM-41 almost only contains high concentration of T_d Ti active sites, which has highest epoxidation activity in these samples. With the decrease of the Ti contents, the sample *120*Si/Ti–MCM-41 has low contents of T_d Ti, which causes the decrease of activity. With the increase of the Ti contents, the most of Ti components existed with O_h state in the sample *30*Si/Ti–MCM-41, which is not active for epoxidation and causes decrease of activity. Moreover, the results in Table 4 show the trend of increased OH and ONE selectivities with the increase of titanium content. It has been reported that the O_h Ti can catalyze the epoxidation of cyclohexene to form OH. And the ONE would be produced by catalytic epoxidation of cyclohexene with anatase titanium oxide. Compared with the sample *60*Si/Ti–MCM-41 prepared from the calcination process and acid treated sample 2.4A-*60*Si/Ti–MCM-41, the results in Table 4 indicate that catalytic activity of these two samples is similar. The sample prepared by template agent extraction method can achieve the same catalytic performance with that of calcination sample.

Fig. 13 compares the cyclohexene conversions and CHE selectivities of the recycled *60*Si/Ti–MCM-41catalysts with those over fresh catalysts. The cylcohexene conversions and CHE selectivities are almost unchanged after recycling for two times. These results demonstrate that the 60Si/Ti–MCM-41 catalysts can be easily regenerated and reused without obvious losses of the catalytic activities in cyclohexene epoxidation.

4. Conclusions

The highly ordered mesoporous molecular sieve Si/Ti–MCM-41 with specific surface area up to 1040 m^2 g^{-1} and pore volume up to 0.74 cm^3 g^{-1} were synthesized from industrial by-product H_2SiF_6. The Si/Ti–MCM-41 sample revealed long range order and regular hexagonal pore structure. Proper selection of the Si/Ti molar ratio, CTAB/Si molar ratio, hydrothermal temperature and time are necessary for the formation of highly ordered mesoporous materials. The over-incorporated titanium content in the Si/Ti–MCM-41 structure deteriorated the mesoporous structure and decreased the

Please cite this article in press as: T. Liu, et al., Synthesis of titanium containing MCM-41 from industrial hexafluorosilicic acid as epoxidation catalyst, Catal. Today (2017), http://dx.doi.org/10.1016/j.cattod.2017.03.011

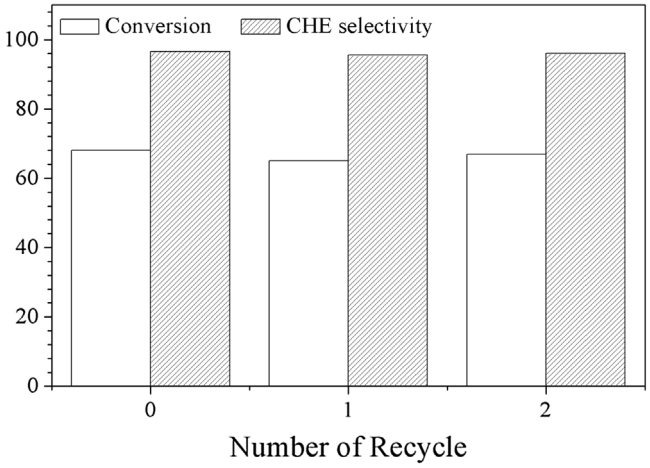

Fig. 13. Catalytic activities of *60*Si/Ti-MCM-41with different number of recycles.

surface area. The amount of CTAB has important influence on the synthesis of MCM-41, the synthesized Si/Ti–MCM-41 own the highest ordered hexagonal *p6 mm* lamellar structure at CTAB/Si molar ratio 0.81 with adjusting the synergy effect of CTAB and silicon. Furthermore, the template agent in the as-synthesis Si/Ti–MCM-41 can be totally dislodged by the 2.4 mol L^{-1} hydrochloric acid anhydrous ethanol solution as the calcinations process. Moreover, the samples xSi/Ti–MCM-41 with Si/Ti molar ratio 60 has the best cyclohexene epoxidation catalytic performance by adjusting the Si/Ti molar. It can be concluded that the T_d Ti atoms in the Si/Ti–MCM-41 is more active for epoxide formation. The catalytic activity of the 60Si/Ti–MCM-41 prepared by extraction template agent method is similar with the 60Si/Ti–MCM-41 prepared by direct calcination. The synthesized catalyst can be recycled for 2 times for epoxidaiton. Therefore, an economical and feasible route has been applied to synthesize Ti contained MCM-41with industrial H_2SiF_6 as silicon sources, which can increase the value-added and bring enormous economic, environmental, and social benefits.

Acknowledgements

The financial supports from Natural Science Foundation, China (NSFC 21306143), Educational Commission of Hubei Province of China (D20161503). Acknowledgement is also extended to Prof. R. Chen of School of chemistry and environmental engineering, Wuhan Institute of Technology for the assistance in UV–vis experiments. Prof. Y. X. Wu is also acknowledged for the support.

References

[1] H.S. Yu, K. Rhee, C.K. Lee, D. Yang, Two-step ammoniation of by-product fluosilicic acid to produce high quality amorphous silica, J. Chem. Eng. 4 (2000) 401–408.
[2] P.B. Sarawade, J. Kim, A. Hilonga, H.T. Kim, Recovery of high surface area mesoporous silica from waste hexafluorosilicic acid (H_2SiF_6) of fertilizer industry, J. Hazard. Mater. 173 (2010) 576–580.
[3] G. Elineema, J.K. Kim, A. Hilonga, G.N. Shao, Y. Kim, D.V. Quang, P.B. Sarawade, H.T. Kim, Quantitative recovery of high purity nanoporous silica from waste products of the phosphate fertilizer industry, J. Ind. Eng. Chem. 19 (2013) 63–67.
[4] G. Cicala, G. Bruno, P. Capezzuto, Plasma deposition of amorphous silicon alloys from fluorinated gases, Pure Appl. Chem. 5 (1996) 1143–1149.
[5] V.V. Guzeev, A.N. D'yachenko, V.N. Grishkov, Integrated utilization of silicon tetrafluoride and zirconium dioxide, Russ. J. Appl. Chem. 76 (2003) 1952–1955.
[6] X. Shen, W. Fan, Y. He, P. Wu, J. Wang, T. Tatsumi, Epoxidation of alkenes and their derivatives over Ti-YNU-1, Appl. Catal. A: Gen. 401 (2011) 37–45.
[7] F. Jin, C. Chang, C. Yang, J. Lee, L. Jang, S. Cheng, New mesoporous titanosilicate MCM-36 material synthesized by pillaring layered ERB-1 precursor, J. Mater. Chem. A 3 (2015) 8715–8724.
[8] C.T. Kresge, J.S. Beck, J.C. Vartuli, W.J. Roth, Ordered mesoporous molecular sieves synthesized by a liquidcrystal template mechanism, J. Am. Chem. Soc. 114 (1992) 710–712.
[9] E. Kraleva, M.L. Saladino, A. Spinella, G. Nasillo, E. Caponetti, $H_3PW_{12}O_{40}$ supported on mesoporous MCM-41 and Al–MCM-41 materials: preparation and characterisation, J. Mater. Sci. 46 (2011) 7114–7120.
[10] Z.Q. Zhang, J. Xiao, L. Dai, Y. Wang, D. Wang, X. Liu, Z. Yan, Synthesis of Al-MCM-41 and FCC diesel hydrorefining study, J. Porous Mat. 19 (2012) 473–479.
[11] N. Marin-Astorga, J.J. Martinez, G. Borda, J. Cubillos, D.N. Suarez, H. Rojas, Control of the chemoselectivity in the oxidation of geraniol over lanthanum, titanium and niobium catalysts supported on mesoporous silica MCM-41, Top. Catal. 55 (2012) 620–624.
[12] Y.L. Xie, Y. Zhang, J. Ouyang, H.M. Yang, Mesoporous material Al-MCM-41 from natural halloysite, Phys. Chem. Miner. 41 (2014) 497–503.
[13] Y.F. Xu, X. Zheng, X. Hu, K.D. Dearn, H.M. Xu, Effect of catalytic esterification on the friction and wear performance of bio-oil, Wear 311 (2014) 93–100.
[14] G. Eimer, S. Casuscelli, G. Ghione, M. Crivello, E. Herrero, Synthesis, characterization and selective oxidation properties of Ti-containing mesoporous catalysts, Appl. Catal. A: Gen. 298 (2006) 232–242.
[15] K. Lin, P.P. Pescarmona, K. Houthoofd, D. Liang, G. Van Tendeloo, P.A. Jacobs, Direct room-temperature synthesis of methyl-functionalized Ti-MCM-41 nanoparticles and their catalytic performance in epoxidation, J. Catal. 263 (2009) 75–82.
[16] F. Jin, S.Y. Chen, L.Y. Jang, J.F. Lee, S. Cheng, New Ti-incorporated MCM-36 as an efficient epoxidation catalyst prepared by pillaring MCM-22 layers with titanosilicate, J. Catal. 319 (2014) 247–257.
[17] C.A. Fyfe, G. Fu, Structure organization of silicate polyanions with surfactants: a new approach to the syntheses, structure transformations, and formation mechanisms of mesostructural materials, J. Am. Chem. Soc. 117 (1995) 9709–9714.
[18] Q.S. Huo, D.I. Margolese, G.D. Stucky, Surfactant control of phases in the synthesis of mesoporous silica-Based materials, Chem. Mater. 8 (1996) 1147–1160.
[19] D. Isabel, F. Mohino, J. Pérez-Pariente, S. Enrique, Synthesis, characterization and catalytic activity of MCM-41-type mesoporous silicas functionalized with sulfonic acid, Appl. Catal. A: G. 205 (2001) 19–30.
[20] H.P. Lin, S. Cheng, C.Y. Mou, Mesoporous molecular sieves MCM-41 with a hollow tubular morphology, Chem. Mater. 10 (1998) 581–590.
[21] V. Antochshuk, A.S. Araujo, M. Jaroniec, Functionalized MCM-41 and Ce-MCM-41 materials synthesized via interfacial reactions, J. Phy. Chem. B 104 (2000) 9713–9719.
[22] M. Adjdir, T. Ali-Dahmane, F. Friedrich, T. Scherer, P.G. Weidler, The synthesis of Al-MCM-41 from volclay – a low-cost Al and Si source, Appl. Clay. Sci. 46 (2009) 185–189.
[23] H. Yang, Y.H. Deng, C.F. Du, S.M. Jin, Novel synthesis of ordered mesoporous materials Al-MCM-41 from bentonite, Appl. Clay. Sci. 47 (2010) 351–355.
[24] F.S. Bastos, O.A. Lima, C. Raymundo, L.D. Fernandes, Mesoporous molecular sieve MCM-41 synthesis from fluoride media, Braz. J. Chem. Eng. 28 (2011) 649–653.
[25] T. Blasco, A. Corma, M.T. Navarro, J.P. Pariente, Synthesis characterization, and catalytic activeity of Ti-MCM-41 structures, J. Catal. 156 (1995) 65–74.
[26] F. Geobaldo, S. Bordiga, A. Zecchina, E. Giamello, DRS UV–vis and EPR spectroscopy of hydroperoxo and superoxo complexes in titanium silicalite, Catal. Lett. 16 (1992) 109–115.
[27] U. Ciesla, F. Schü, Ordered mesoporous materials, Micropor. Mesopor. Mat. 27 (1999) 131–149.
[28] P.T. Tanev, M. Chibwe, T.J. Pinnavaia, Titanium-containing mesoporous molecular sieves for catalytic oxidation of aromatic compounds, Nature 368 (1994) 321–323.
[29] Elliott P. Barrett, Leslie G. Joyner, Paul P. Halenda, The determination of pore volume and area distributions in porous substances, J. Am. Acad. Audial. 73 (1951) 373–380.
[30] M. Thommes, K. Kaneko, A.V. Neimark, J.P. Olivier, F. Rodriguez-Reinoso, J. Rouquerol, K.S.W. Sing, Physisorption of gases, with special reference to the evaluation of surface area and pore size distribution (IUPAC Technical Report), Pure Appl. Chem. 87 (2015) 1051–1069.
[31] R. Peng, D. Zhao, N.M. Dimitrijevic, T. Rajh, R.T. Koodali, Room temperature synthesis of Ti–MCM-48 and Ti–MCM-41 mesoporous materials and their performance on photocatalytic splitting of water, J. Phy. Chem. C 116 (2012) 1605–1613.
[32] C.P. de Macedo, C.A.B. Negrão, L.G.M. de Macedo, J.R. Zamian, G.N. Da Rocha Filho, C.E.F. Da Costa, Kinetic study of template removal of Al-MCM-41 synthesized at room temperature, J. Therm. Anal. Calorm. 115 (2014) 31–36.
[33] N.N. Opembe, E. Vunain, A.K. Mishra, K. Jalama, R. Meijboom, Thermal stability of ti–MCM-41, J. Therm. Anal. Calorim. 117 (2014) 701–710.
[34] C.W. Ingram, T. Mehreteab, J. Liesen, I. Harruna, Enhanced expoxidation activity of Ti-mesoporous catalysts containing organic–inorganic porewall, J. Porous Mat. 20 (2013) 143.

Please cite this article in press as: T. Liu, et al., Synthesis of titanium containing MCM-41 from industrial hexafluorosilicic acid as epoxidation catalyst, Catal. Today (2017), http://dx.doi.org/10.1016/j.cattod.2017.03.011